Pergamon

Int. J. Multiphase Flow Vol. 22, No. 2, pp. 325–333, 1996

0301-9322(95)00065-8
0301-9322/96 $15.00 + 0.00

ON THE NATURE OF EPHEMERAL WAVES IN VERTICAL ANNULAR FLOW

A. WOLF[1], S. JAYANTI[2] and G. F. HEWITT[1]

[1]Department of Chemical Engineering, Imperial College, London SW7 2BY, U.K.

[2]Department of Chemical Engineering, Indian Institute of Technology, Madras 600 036, India

(*Received 15 March 1994; in revised form 4 September 1995*)

Abstract—Flow visualization experiments and film thickness measurements were conducted in air–water upward annular flow in a tube of 31.8 mm i.d. As the liquid flow rate was increased at a constant gas flow rate, first disturbance waves and then ephemeral waves were found to occur on the liquid film. A model to determine the film Reynolds number has been developed, and is used to show that the onset of disturbance waves and of ephemeral waves happens at a substrate film Reynolds number of about 500. It is proposed that the ephemeral waves are none but developing disturbance waves.

Key Words: gas–liquid flow, annular flow, two-phase flow, waves

1. INTRODUCTION

In vertical gas–liquid annular flow, part of the liquid phase flows in the form of a thin liquid film and the rest in the form of droplets in the gas core. It is traditionally thought that the interface is covered with two types of waves: ripple waves, which are small amplitude, short-lived waves; and disturbance waves, which have an amplitude of about five times the mean film thickness and are coherent over long axial distances (Hewitt & Hall-Taylor 1970). A third type of wave has been reported by Sekoguchi *et al.* (1985) and Sekoguchi & Takeishi (1989). These are the so-called "ephemeral waves" which have an amplitude comparable to the disturbance waves but have a smaller velocity, and are shorter-lived in the sense that they are not axially coherent over long distances (due to their being overtaken by the regular disturbance waves). Sekoguchi *et al.* obtained pictures of these ephemeral waves by computer reconstruction of the interface structure measured by a large cluster of conductance probes. They found that these ephemeral waves are produced at high liquid flow rates. The purpose of the present paper is to report *visual* observation of these ephemeral waves in vertical annular flow, and to present a hypothesis concerning the nature of these waves.

2. OBSERVATION OF EPHEMERAL WAVES

Air–water upward annular flow experiments were conducted in an 11 m-long pipe of 31.8 mm i.d. The film structure was observed using a visualization section located at a distance of 10.2 m from the porous sinter through which water was introduced. The visualization section was made of fluorinated ethylene propylene which has a refractive index nearly equal to that of water (Hewitt *et al.* 1990) which enabled visualization of thin films in pipes. The flow was photographed using a video camera operating at 50 frames per second. Two strobelights, each giving a flash lasting only 20 μs, were used synchronously with the video camera. This gave an effective filming rate of 50,000 frames per second, which was enough to get a clear picture of the interface at low gas flow rates. Film thickness was measured using conductance probes located at about the same axial location. The conductance probes were of concentric type (Hewitt 1982) but with the modification of Chan (1990) of using a concentric cylinder as the earth rather than the pipe wall. Two sets of conductance probes were placed 0.11 m apart to cross-correlate the film thickness and thereby obtain wave velocities. The probes were operated at a sampling rate of 1000 Hz, and the results were stored in a computer for later analysis. Film thickness measurements were conducted in the

following ranges: liquid mass flux varying between 10 and 120 kg/m^{2}s and gas mass flux varying between 72 and 164 kg/m^{2}s. The pressure at the visualization section was 1.83 bar giving an air density of 2.14 kg/m^3. The visualization studies were perfomed in a smaller range of gas flow rates (up to 55 kg/m^{2}s) because the picture quality deteriorated at higher flow rates. It must be noted that one cannot get the same detailed and localized information from the conductance probes as from the visualization technique whereas the latter cannot give any quantitative indication of the film height. However, both the techniques can be used to measure the frequency and the velocity of the disturbance waves, and some measurements and visualizations were carried out simultaneously to verify that they gave consistent results.

The main observations from the experiments were as follows: below a certain critical liquid mass flux (in this case 10 kg/m^{2}s), disturbance waves occurred very rarely, if at all, and only ripple waves were present. For a liquid mass flux between 10 and 20 kg/m^{2}s, disturbance waves were observed very irregularly, and above this flow rate they appeared fairly regularly. A typical ripple wave region and a typical disturbance wave region observed under these conditions are shown in figure 1(A) and (B), respectively. The pictures are taken such that one is looking at the tube from the outside. The bright white patch is due to the reflection of the light source and should be disregarded. In figure 1, the tube wall is covered by a wavy film. However, in figure 1(B), the undulations in the middle of the picture (as marked) are stronger and more coherent around the circumference and are characteristic of the disturbance wave region. The transition from this squally disturbance wave region to the ripple region (where the liquid film appears to be much smoother) is quite sudden and is clearly marked. In disturbance wave-free annular flow, the film structure is uniformly slightly rough [as in figure 1(A)], whereas when disturbance waves are occurring, there are regions where the film appears much rougher [figure 1(B)].

At even higher liquid flow rates, smaller patches of disturbed film region appeared between successive disturbance waves. These are, presumably, the "ephemeral" waves of Sekoguchi *et al.* (1985) and are illustrated in figure 2(A). Here, a small patch of roughened film, of a width of about one-fifth of the tube diameter, appears in the centre of the picture. The texture of the roughness is similar to that in the disturbance wave region occurring under the same conditions shown in figure 2(B). The flow conditions for the appearance of these ephemeral waves agree well with those

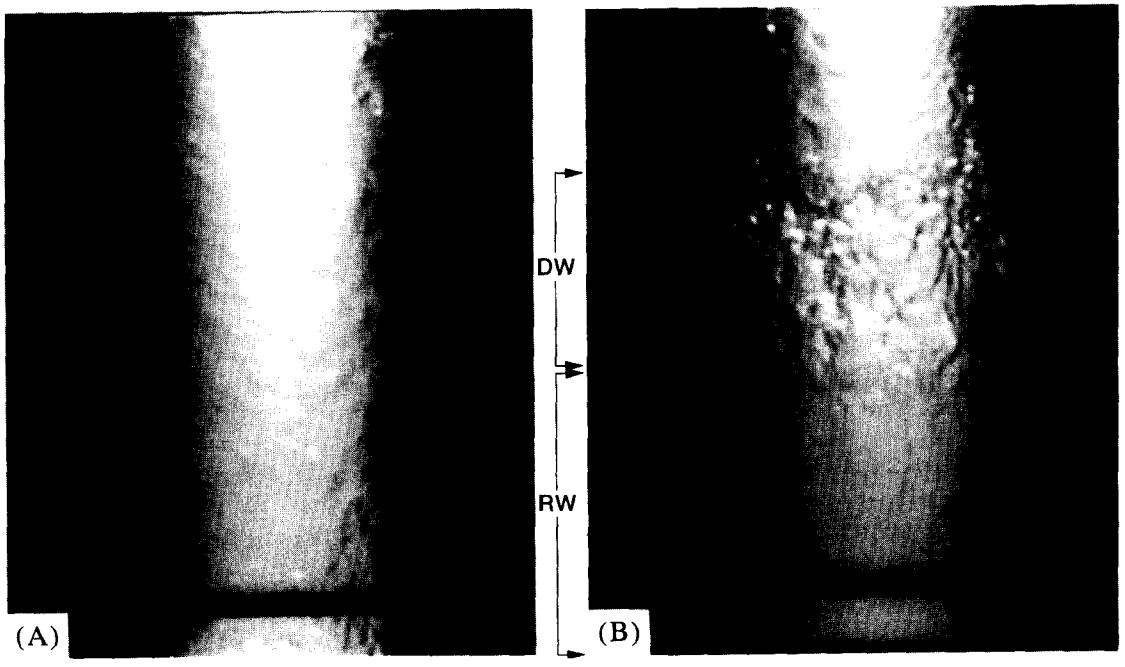

Figure 1. A typical (A) ripple wave region and (B) disturbance wave region in upward annular flow. Air flow rate = 45.4 kg/m^{2}s and water flow rate = 21.2 kg/m^{2}s; air density = 1.41 kg/m^3. DW = disturbance wave region; RW = ripple wave region.

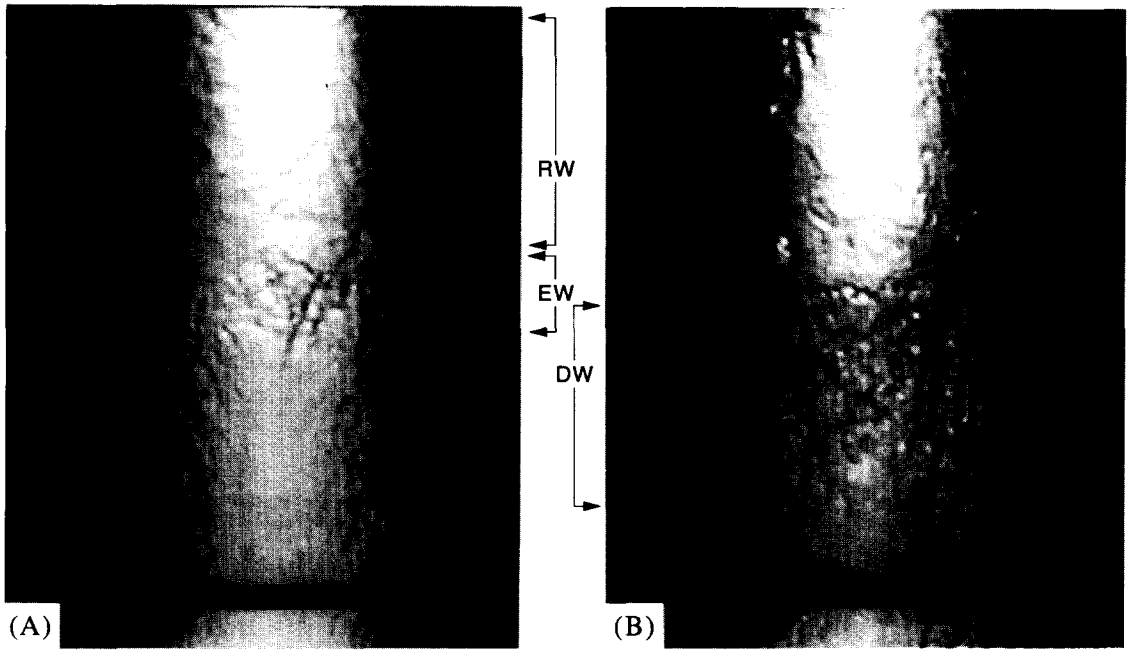

Figure 2. A typical (A) ephemeral wave in upward annular flow at an air flow rate of 50.1 kg/m²s, water flow rate of 103.1 kg/m²s and air density of 1.64 kg/m³. (B) Typical disturbance wave occurring under the same flow conditions. DW = disturbance wave region; EW = ephemeral wave region; RW = ripple wave region.

of Sekoguchi & Takeishi (1989). Apart from the differences in the width of the roughened region, which is typically of the order of one tube diameter for disturbance waves, these two types of rough patches also differ in their circumferential coherence (the ephemeral waves being less coherent and having a streaky appearance) and in the speed at which they move along the pipe. The ephemeral waves travel at a considerably lower velocity than the disturbance waves. This is illustrated in figure 3 which shows two successive frames (20 ms apart) of the motion of an ephemeral wave with a disturbance wave behind it. The distance between the two is shorter in figure 3(B) than in figure 3(A). The velocity of the ephemeral waves estimated from this picture is 1.7 m/s and that of the disturbance waves is 3 m/s (which agrees well with the value of 3.1 m/s obtained by cross-correlating the film thickness signals from the conductance probes). Due to this velocity difference, coalesecence of the two types of waves occurs. As a result, the disturbance wave size (in terms of their width) varies significantly when ephemeral waves occur. Figure 4 shows a disturbance wave region of a width of nearly one and a half tube diameters, again occurring under the same flow conditions as those in figure 3. [Figure 4 also brings out very clearly the squally appearance of the liquid film in the disturbance wave region which is well-supported by the computer-reconstructed picture in figure 6(A) of Sekoguchi & Takeishi (1989).] In contrast, the disturbance waves at lower liquid flow rates (where there are no ephemeral waves) have a fairly constant width for a set of flow conditions. This can be used as a means of detecting if ephemeral waves occur.

The above observations are based on visualization studies. The film thickness traces used in the present study cannot give such a detailed picture of the interface due to the spatial averaging inherent in the technique. A typical film thickness trace obtained in the present experiments is shown in figure 5(A). It can be seen that it does not reflect very well the true nature of the alternating interface texture of the relatively smooth ripple wave region and the rough disturbance wave region seen in figures 1 and 2. The power spectrum of the film thickness trace [figure 5(B)] shows that the interfacial waves are aperiodic and irregular and that they do not have a constant frequency. Even the probability density function of the film thickness trace [figure 5(C)] is unable to clearly distinguish the nature of disturbance waves. The maximum probablity here corresponds to the substrate film thickness, and since disturbance waves do not have a constant height and their height is underestimated by conductance probes, they cannot be clearly distinguished in the

probability density function, as pointed out by Schadel & Hanratty (1989). (Even if it were possible to measure the local height precisely, the variation of the liquid film height within the disturbance wave region would be such that they could not be distinguished on a probability density function plot.) Thus, traditional methods of statistical and spectral analysis of film thickness traces obtained from conductance probe techniques are unable to reproduce the true nature of the interfacial structure. However, they can be used to measure the frequency and velocity of these waves.

3. CONDITIONS IN WHICH EPHEMERAL WAVES OCCUR

The origin of the ephemeral waves is not known; however, they resemble the disturbance waves in more than mere appearance in the sense that, like disturbance waves, they do not seem to appear unless the liquid flow rate is sufficiently high. Film thickness measurements using the conductance

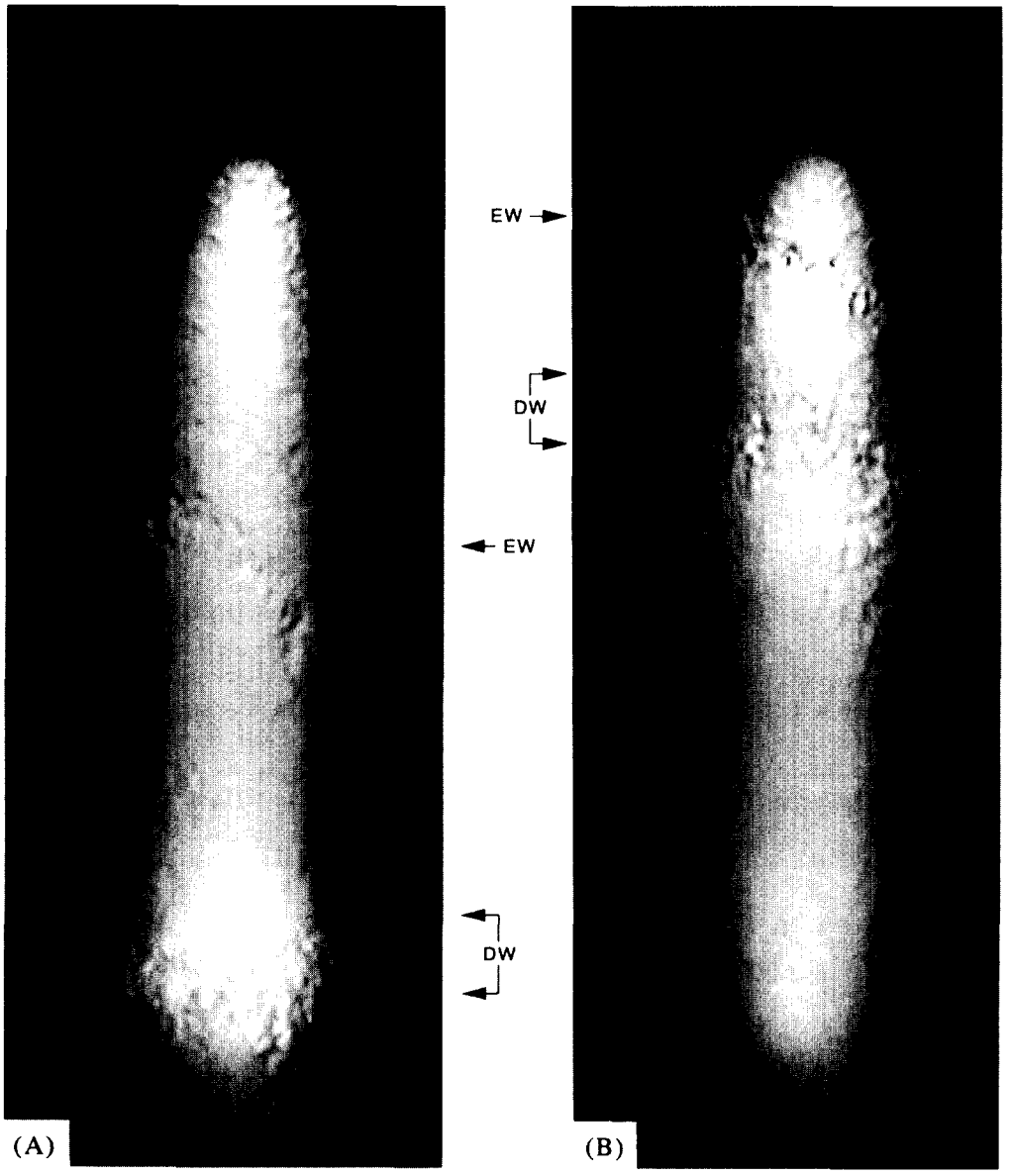

Figure 3. (A) and (B). Successive frames (0.02 s apart) showing the relative speeds of the disturbance wave and the ephemeral wave. Air flow rate = 50.1 kg/m^{2}s, water flow rate = 103.1 kg/m^{2}s and air density = 1.64 kg/m^3. DW = disturbance wave region; EW = ephemeral wave region.

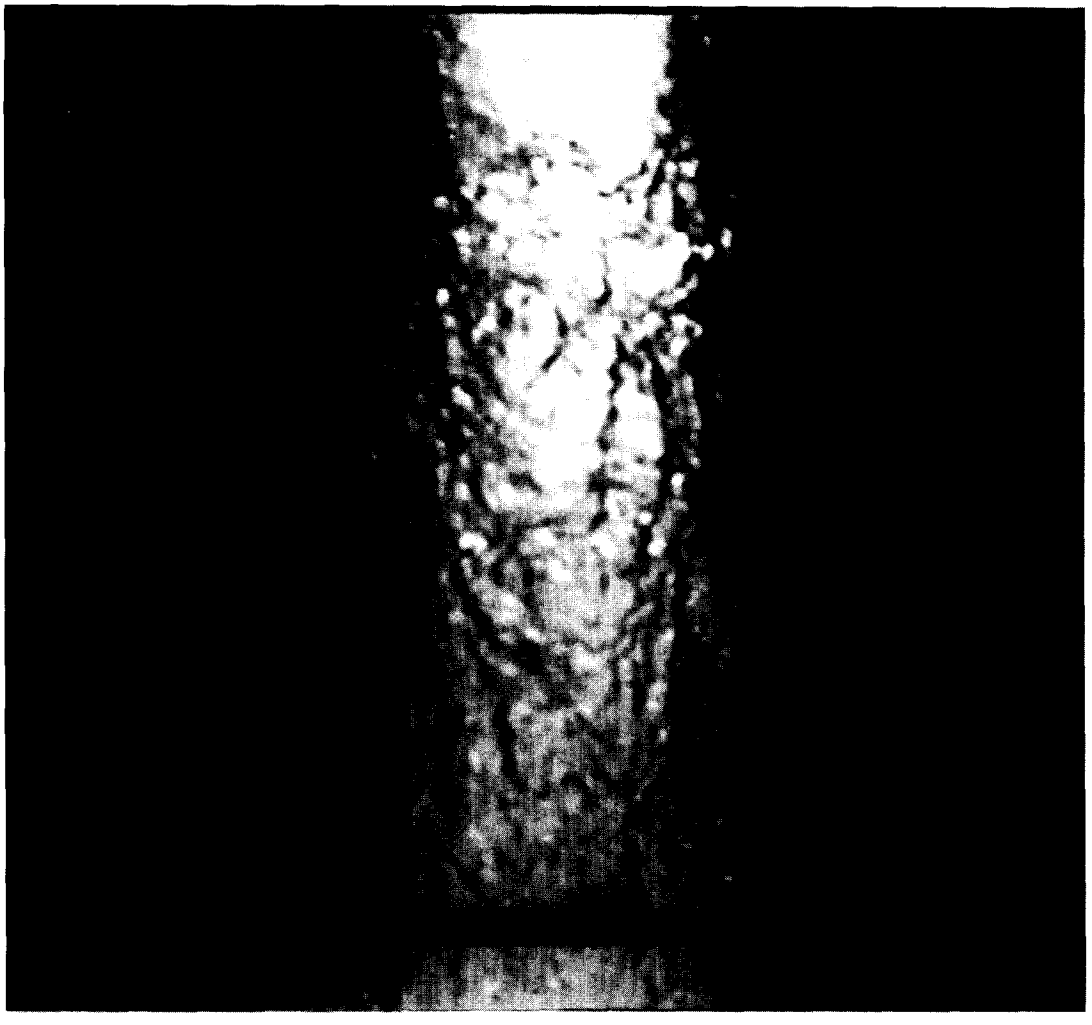

Figure 4. A large disturbance wave [cf. Figure 2(B)] occurring presumably due to the coalescence of a disturbance wave and an ephemeral wave. Air flow rate = 50.1 kg/m^{2}s, water flow rate = 103.1 kg/m^{2}s and air density = 1.64 kg/m^3.

probe show that the substrate film thickness increases as the liquid flow rate is increased at a constant gas flow rate. Since this substrate film is driven mainly by the interfacial shear, the film flow rate and hence the film Reynolds number, increase as the liquid flow rate increases. Thus it is possible that, just as in the case of disturbance waves, there is a critical substrate film Reynolds number above which ephemeral waves are formed (Asali *et al.* 1985; Owen 1986; Schadel 1988). In the present study, a model is constructed to estimate the liquid film Reynolds number given its thickness, and this model is used to verify if there exists a critical Reynolds number for the onset of ephemeral waves.

The model is based on the equivalence between the substrate film in between disturbance waves and a film of the same thickness flowing in a disturbance wave-free annular flow, both having the same geometry, fluids and superficial gas velocity. The basis for this equivalence is that the substrate film thickness is very small compared to the other length scales in annular flow so that its motion will be governed by local conditions, which in this case are the film thickness and the gas flow (the driving force) characteristics, namely, gas density, viscosity, velocity and the tube diameter. With this approximation, we can make use of the data of Shearer & Nedderman (1965), who conducted experiments in annular flow without disturbance waves (the liquid flow rate being less than that required to generate disturbance waves) to determine the interfacial friction factor and hence the substrate film Reynolds number. This is done as follows.

Since the spacing between successive disturbance waves is very long compared to the film thickness, we can assume that the flow in the substrate film is fully developed. The flow here is laminar and the film thickness (δ) is very small (of the order of 0.1 mm); therefore the shear stress can be assumed to be constant across the film. In such a case, the film thickness, the interfacial shear stress (τ_i) and the volumetric flow rate (Q) per unit perimeter are related as follows (Shearer & Nedderman 1965):

$$\delta^2 = \frac{8\mu_L Q}{D}\frac{L}{\Delta p} \quad [1]$$

$$\tau_i = \frac{1}{2} f_i \rho_G U_G^2 = \frac{D}{4}\frac{\Delta p}{L} \quad [2]$$

so that

$$\delta = \sqrt{\frac{2\mu_L Q}{\tau_i}}. \quad [3]$$

Here, D is the tube diameter, μ_L the liquid viscosity, f_i is the interfacial friction factor, ρ_G the gas density, U_G the mean gas velocity and $\Delta p/L$ the pressure gradient. Since the film Reynolds number, $Re_{Lf} = 4\rho_L Q/\mu_L$, is proportional to Q, equation [3] expresses a functional relationship between the film thickness, film Reynolds number and the interfacial shear stress. Shearer & Nedderman (1965) obtained data of the pressure gradient, film thickness and film flow rate under air–water ripple flow conditions in a pipe of 31.8 mm i.d. (which is the same as that of the present set of experiments), and presented a dimensional correlation between the film Reynolds number and the equivalent sand grain roughness at the interface. These data have been used in the present study to develop the following explicit and dimensionless correlation between the interfacial friction factor, the film thickness and the gas Reynolds number:

$$\frac{f_i}{f_G} = 0.856 + 0.00281 Re_G \frac{\delta}{D} \quad [4]$$

where Re_G is the gas phase Reynolds number based on the superficial gas velocity and the tube diameter, and f_G is the gas phase friction factor for flow in a smooth tube. It should be noted that this correlation cannot apply, of course, in the limit of δ approaching zero (i.e. zero film flow rate), but it suits the purpose of the present calculations.

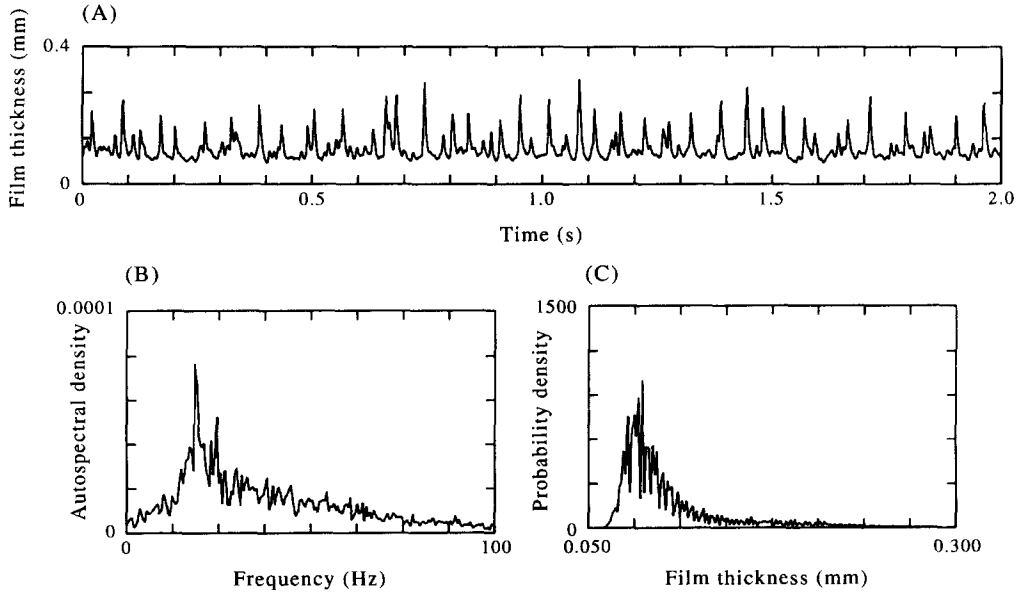

Figre 5. (A) Film thickness trace at an air flow rate of 98 kg/m^{2}s; water flow rate of 40 kg/m^{2}s and air density of 2.14 kg/m^3. (B) Autospectral density of the film thickness trace in (A). (C) Probability density function of the film thickness trace in (A).

Table 1. Substrate film thickness and Reynolds number for various flow conditions

Gas superficial velocity U_G (m/s)	Liquid superficial velocity U_L (m/s)	Substrate film thickness δ (mm)	Substrate film Reynolds number Re_{Lf}
33.5	0.02	0.109	260
	0.04	0.124	370
	0.06	0.141	510
	0.08	0.142	520
	0.10	0.145	550
	0.12	0.145	550
45.6	0.01	0.074	200
	0.02	0.080	245
	0.04	0.082	265
	0.06	0.086	300
	0.08	0.09	330
	0.10	0.103	480
	0.12	0.103	480
60.5	0.01	0.059	220
	0.02	0.062	250
	0.04	0.067	305
	0.06	0.075	415
	0.08	0.074	400
	0.10	0.079	470
	0.12	0.085	585

Thus, if the film thickness of the substrate and the gas velocity are known, the substrate film Reynolds number can be calculated using the above relation. In principle, it should be relatively straightforward to obtain the substrate film thickness values for the various flow rates because the film thickness was measured at a sampling rate of 1000 Hz. However, as shown in figure 5, the variation of the film thickness, as measured by the conductance probes, with time does not follow the idealized picture consisting of alternate regions of smooth ripple wave region and rough disturbance wave region and the interfacial waves are aperiodic and irregular. It is therefore necessary to use a statistical method to obtain an objective estimate of the substrate film thickness. The method followed in the present study is to construct a probability density function of the film thickness trace [figure 5(C)] and to take the film thickness corresponding to the maximum probability as the substrate film thickness.

The substrate film thickness thus obtained for a range of air and water mass fluxes is given in table 1. Also given are the corresponding film Reynolds numbers calculated as described above. It is seen that the substrate film thickness increases with increasing liquid flow rate and that it reaches a fairly steady value at a Reynolds number of about 500. (Given the aperiodic nature of the waves, the values in table 1 should not be taken as exact; for example, the film thickness is not measured to an accuracy of 1 μm, but the trend with increasing liquid flow rate is clearly established.) This is also the point at which the waves on the film become continuous, presumably, due to the formation of ephemeral waves between successive disturbance waves. This is illustrated in figure 6 where film thickness traces at three liquid flow rates measured at a constant gas flow rate are plotted as a function of time. In figure 6(A), there is a clear demarcation between between disturbance waves and the ripple wave region in between. Also, the base of the disturbance wave peak is roughly constant in all cases. In figure 6(B), there is a larger variation of the wave height and the base width indicating the presence of ephemeral waves, and some of the likely ones are marked in the figure. However, a substrate layer still exists. In contrast, the film thickness trace in figure 6(C) is continuously wavy and a clearly-defined substrate layer is no longer present. A number of waves with a wide base, presumably due to the more frequent coalescence of disturbance and ephemeral waves, occur. It thus appears that as the liquid flow rate increases from a low value, the substrate film Reynolds number increases up to a critical value of around 500 at which ephemeral waves are formed on the substrate film between successive disturbance waves. It is interesting to note that this critical value is roughly the same as that for the appearance of disturbance waves, thus indicating a similarity between the two.

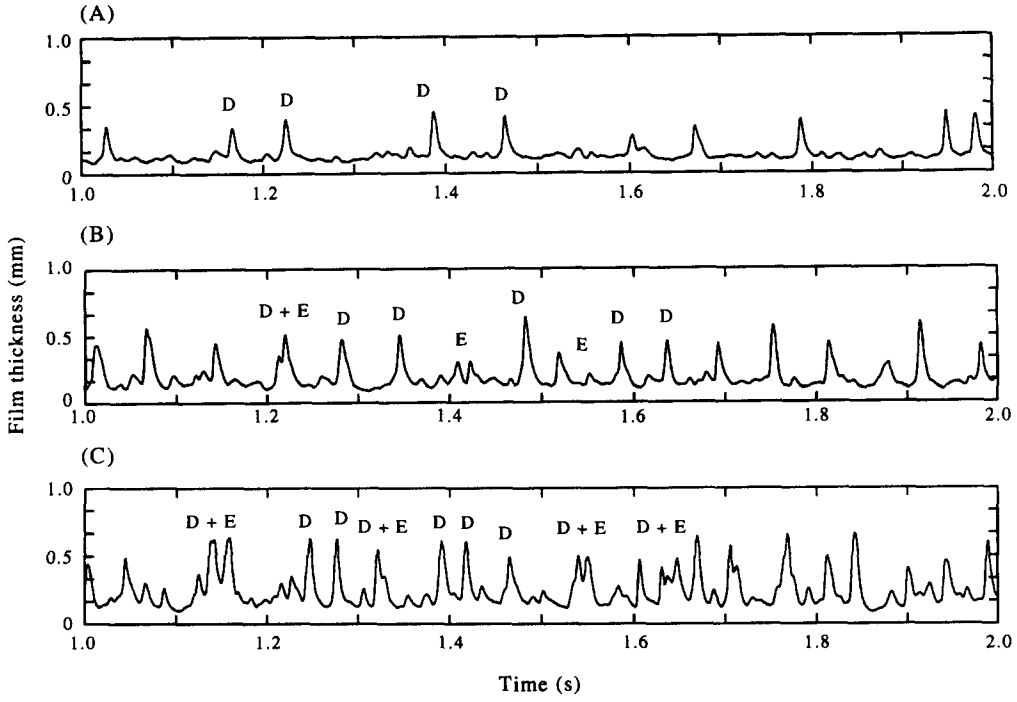

Figure 6. Film thickness trace at an air flow rate of 72 kg/m²s, air density of 2.14 kg/m³ and a water flow rate of (A) 20 kg/m²s; (B) 60 kg/m²s and (C) 100 kg/m²s. DW = disturbance wave region; EW = ephemeral wave region.

4. DISCUSSION

The flow visualizations experiments described in show that regular disturbance waves are formed when the film Reynolds number is of the order of 500. As the liquid flow rate increases (at the same gas flow rate), no new waves are formed until a threshold is reached at which the so-called "ephemeral waves" are formed between disturbance waves. These new waves are similar in structure to the disturbance waves, but move much more slowly. As a result of this, they are overtaken by the latter and appear to be short-lived.

A model, which is based on the equivalence of the substrate film flow and that in a disturbance wave-free annular flow of the same mean film thickness and the gas velocity, has been developed to calculate the substrate film Reynolds number from measured substrate film thickness values. It is shown that the when disturbance waves are present, and when the liquid flow rate is low, the substrate film Reynolds number is small. It increases with increasing liquid flow rate, and reaches a maximum value of about 500 after which the film thickness trace becomes continuous and a clear substrate layer does not exist due to the formation of regular ephemeral waves between disturbance waves. Since disturbance waves also have approximately the same lower limit on the film Reynolds number, this may mean that ephemeral waves are none but developing disturbance waves.

It is interesting to speculate on the mechanism(s) of the buildup of the substrate film between disturbance waves. There will be some liquid film left behind by a disturbance wave. At low liquid flow rates, this should be the primary source of the liquid in the substrate. As the liquid flow rate is increased, a significant part of it flows in the form of droplets which are entrained from the crests of the disturbance waves. Since the deposition of the droplets is governed, to a large extent, by diffusional processes, they would be redeposited not only in the disturbance wave region but also on the substrate. Since there can be no entrainment from the substrate film, this depositon constitutes a net influx of liquid into the substrate and may contribute to its buildup. Since droplet concentration in the core increases rapidly with increasing liquid flow rate, this would be an important factor at high liquid flow rates. A combination of both mechanisms is likely to be responsible for the substrate film flow rate and hence for the occurrence or not of ephemeral waves.

Acknowledgement—S. Jayanti and A. Wolf gratefully acknowledge the financial support received from the Science and Engineering Research Council during the course of this study.

REFERENCES

Asali, J. C., Hanratty, T. J. & Andreussi, P. 1985 Interfacial drag and film height for vertical annular flow. *AIChE J.* **31,** 895–902.

Chan, G. T. W. C. 1990 Evaporation and condensation in annular vertical upward flow. Ph.D. thesis, Imperial College, University of London, England.

Hewitt, G. F. 1982 Measurement techniques. In *Handbook of Multiphase Systems* (Edited by Hetsroni, G.), Chapter. 10. Hemisphere, Washington, DC.

Hewitt, G. F. & Hall-Taylor, N. S. 1970 *Annular Two-phase Flow*. Pergamon Press, Oxford.

Hewitt, G. F., Jayanti, S. & Hope, C. B. 1990 Structure of thin liquid films in gas–liquid horizontal flow. *Int. J. Multiphase Flow* **16,** 951–957.

Owen, D. G. 1986 An experimental and theoretical analysis of equilibrium annular flows. Ph.D. thesis, University of Birmingham, England.

Schadel, S. A. 1988 Atomization and deposition rates in vertical annular two-phase flow. Ph.D. thesis, University of Illinois, Urbana, IL.

Schadel, S. A. & Hanratty, T. J. 1989 Interpretation of atomization rates of the liquid film in gas–liquid annular flow. *Int. J. Multiphase Flow* **15,** 893–900.

Sekoguchi, K. & Takeishi, M. 1989 Interfacial structures in upward huge wave flow and annular flow regimes. *Int. J. Multiphase Flow* **15,** 295–305.

Sekoguchi, K., Takeishi, M. & Ishimatsu, T. 1985 Interfacial structure in vertical upward annular flow. *Physicochem. Hydrodynam.* **6,** 239–255.

Shearer, C. J. & Nedderman, R. M. 1965 Pressure gradient and liquid film thickness in co-current upwards flow of gas–liquid mixtures: application to film cooler design. *Chem. Engng Sci.* **20,** 671–683.